Isolation and pharmacological characterisation of δ-atracotoxin-Hv1b, a vertebrate-selective sodium channel toxin

Tim H. Szeto[b,1], Liesl C. Birinyi-Strachan[a,1], Ross Smith[d], Mark Connor[c], Macdonald J. Christie[c], Glenn F. King[b], Graham M. Nicholson[a,*]

[a] *Department of Health Sciences, University of Technology, Sydney, P.O. Box 123, Broadway, N.S.W. 2007, Australia*
[b] *Department of Biochemistry, University of Connecticut Health Center, Farmington, CT 06032, USA*
[c] *Department of Pharmacology, University of Sydney, Sydney, N.S.W. 2006, Australia*
[d] *Department of Biochemistry, University of Queensland, Brisbane, Qld. 4072, Australia*

Received 9 February 2000

Edited by Maurice Montal

Abstract δ-Atracotoxins (δ-ACTXs) are peptide toxins isolated from the venom of Australian funnel-web spiders that slow sodium current inactivation in a similar manner to scorpion α-toxins. We have isolated and determined the amino acid sequence of a novel δ-ACTX, designated δ-ACTX-Hv1b, from the venom of the funnel-web spider *Hadronyche versuta*. This 42 residue toxin shows 67% sequence identity with δ-ACTX-Hv1a previously isolated from the same spider. Under whole-cell voltage-clamp conditions, the toxin had no effect on tetrodotoxin (TTX)-resistant sodium currents in rat dorsal root ganglion neurones but exerted a concentration-dependent reduction in peak TTX-sensitive sodium current amplitude accompanied by a slowing of sodium current inactivation similar to other δ-ACTXs. However, δ-ACTX-Hv1b is approximately 15–30-fold less potent than other δ-ACTXs and is remarkable for its complete lack of insecticidal activity. Thus, the sequence differences between δ-ACTX-Hv1a and -Hv1b provide key insights into the residues that are critical for targeting of these toxins to vertebrate and invertebrate sodium channels.

Key words: Funnel-web spider toxin; δ-Atracotoxin; Sodium channel; Scorpion toxin

1. Introduction

Australian funnel-web spiders (Araneae: Hexathelidae: Atracinae) belong to the infraorder Mygalomorphae and are distributed mainly along the southeastern seaboard. The funnel-web spider sub-family, Atracinae, comprises around 35 species divided between the genera *Atrax* and *Hadronyche*. A variety of peptides known as atracotoxins (ACTXs) have been isolated from the venom of these spiders, particularly the Blue Mountains funnel-web spider *Hadronyche versuta* (Rainbow). These toxins include the ω-ACTXs, which selectively inhibit insect voltage-gated calcium channels [5,25], ACTX-Hvf17, a peptide with strong sequence homology to mamba intestinal toxin [23], and more recently the insecticidal J-ACTXs with as yet unknown molecular targets (G.F.K. et al., unpublished results). However, the potentially lethal toxins responsible for the major primate-specific symptoms of envenomation, δ-ACTX-Hv1 (formerly versutoxin) from *H. versuta* [2] and its homologue δ-ACTX-Ar1 (formerly robustoxin) from *Atrax robustus* [21], have been shown to target the voltage-gated sodium channel.

δ-ACTX-Ar1 and -Hv1 are highly homologous 42 residue peptides with 83% amino acid identity and only two non-conserved substitutions. They show no significant sequence homology with any presently known neurotoxins. The toxins have a high proportion of basic residues and they are cross-linked by four conserved intramolecular disulfide bonds (see Fig. 2). Recent work has revealed that both δ-ACTX-Ar1 and -Hv1 exert their neurotoxic actions by slowing tetrodotoxin (TTX)-sensitive sodium current inactivation [14,15], an action similar to scorpion α-toxins and sea anemone toxins [8,22]. Indeed, nanomolar concentrations of δ-ACTX-Ar1 and -Hv1 completely inhibit the binding of the classical scorpion α-toxins Lqh II (from the scorpion *Leiurus quinquestriatus hebraeus*) and Aah II (from the scorpion *Androctonus australis hector*) to neurotoxin receptor site 3 on rat brain sodium channels [11,12]. Interestingly, however, δ-ACTXs also inhibit the binding of the scorpion α-insect toxin LqhαIT to cockroach neuronal membranes and produce a delayed contractile paralysis in insects similar to LqhαIT. Thus, δ-ACTXs represent a new class of toxins which bind to both mammalian and insect sodium channels at sites similar to, or partially overlapping with, neurotoxin receptor site 3.

The three-dimensional solution structures of δ-ACTX-Hv1 [4] and δ-ACTX-Ar1 [17] have been determined using NMR spectroscopy. Both display a small triple-stranded antiparallel β-sheet and a cystine knot which places them in a class of toxins and inhibitory polypeptides with an 'inhibitor cystine knot' [18]. Interestingly, the protein scaffold is distinctly different to that of the scorpion α-toxins Aah II [6] and LqhαIT [24] and the sea anemone toxin anthopleurin-B [13] despite similar actions of all three toxins on sodium current inactivation [3,8,22]. However, the three groups of toxins share a number of topologically related anionic and cationic residues.

*Corresponding author. Fax: (61)-2-9514 2228.
E-mail: graham.nicholson@uts.edu.au

[1] Equal contributions.

Abbreviations: δ-ACTX-Ar1, δ-atracotoxin-Ar1 (formerly robustoxin) from *Atrax robustus*; δ-ACTX-Hv1b, δ-atracotoxin-Hv1a (formerly versutoxin) from *Hadronyche versuta*; TTX, tetrodotoxin; Aah II, anti-mammal α-toxin from the scorpion *Androctonus australis hector*; LqhαIT, α-insect toxin from the scorpion *Leiurus quinquestriatus hebraeus*; TFA, trifluoroacetic acid; rpHPLC, reverse-phase high performance liquid chromatography; HEPES, *N*-2-hydroxyethylpiperazine-*N*-2-ethanesulfonic acid; DRG, dorsal root ganglion; TEA, tetraethylammonium; PTH, phenylthiohydantoin

PII: S0014-5793(00)01339-9

This allowed the construction of a plausible molecular model, based on electrostatic complementarity, to explain how all of these toxins might interact with a patch of charged residues within the S3–S4 loop of domain IV of the voltage-gated sodium channel [19].

Here, we describe the isolation and pharmacological characterisation of a novel δ-ACTX from the venom of *H. versuta*. This toxin is a much less potent modulator of vertebrate sodium channels that previously characterised δ-ACTXs and, in marked contrast to δ-ACTX-Hv1 and δ-ACTX-Ar1, it completely lacks insecticidal activity. The actions of this toxin provide further support for the role of N-terminal cationic residues in determining phylogenetic specificity.

2. Materials and methods

2.1. Toxin purification and sequencing

Venom was collected from both male and female Blue Mountains funnel-web spiders (*H. versuta*) and fractionated using reverse-phase high performance liquid chromatography (rpHPLC) exactly as reported previously [3]. Prior to biochemical analyses, δ-ACTX-Hv1b (peak b in Fig. 1B) was further purified on an analytical C_{18} rpHPLC column using a gradient of 5–29% CH_3CN/0.1% trifluoroacetic acid (TFA) over 5 min, then 29–32% CH_3CN/0.1% TFA over 15 min, at a flow rate of 0.75 ml/min. Purified toxin was collected, lyophilised and stored at −20°C until required. Toxin quantification was performed using a bicinchoninic acid Protein Assay kit (Pierce, Rockford, IL, USA) using bovine serum albumin as a standard. Absorbances were read at 570 nm on a Bio-Rad Model 450 microplate reader. The molecular mass was determined by electrospray ionisation mass spectrometry.

In preparation for amino acid sequencing, the toxin was reduced and cysteine residues were pyridylethylated as described previously [3]. The reduced, pyridylethylated toxin was purified using rpHPLC as described previously [3], then the entire peptide sequence was obtained from a single sequencing run on an Applied Biosystems/Perkin Elmer Procise 492 cLC protein sequencer.

2.2. Rat vas deferens bioassay

Peptide toxins were assayed for their effect in rat vas deferens nerve muscle tissue as described previously [3]. Twitch contractions of these muscles were elicited by field stimulation of the nerve [3], and muscular contractions were recorded using an isometric force transducer and displayed on a flatbed chart recorder. Contractions of each tissue were recorded in the absence of additives or following injection of peptides (10–20 μl in water) directly into the bath buffer. δ-ACTX-Hv1 (100 nM) was used as a positive control.

2.3. Electrophysiological studies

Acutely dissociated dorsal root ganglion (DRG) neurones were prepared from 4–12 day old Wistar rats and maintained in short-term primary culture using the method described by Nicholson et al. [15]. Voltage-clamp recordings were made with whole-cell patch-clamp techniques [7] using an AxoPatch 200A patch-clamp amplifier (Axon Instruments, Foster City, CA, USA). Micropipettes were pulled from borosilicate glass capillary tubing (Corning 7052 Glass, Warner Instruments) and had d.c. resistances of 0.8–2.0 MΩ.

To record macroscopic sodium currents, micropipettes were filled with a solution of the following composition (in mM): CsF 135, NaCl 10, *N*-2-hydroxyethylpiperazine-*N*-2-ethanesulfonic acid (HEPES) 5, with the pH adjusted to 7.0 with 1 M CsOH. The external bathing solution contained (in mM): NaCl 30, $MgCl_2$ 1, $CaCl_2$ 1.8, CsCl 5, KCl 5, D-glucose 25, HEPES 5, tetraethylammonium (TEA) chloride 20, tetramethylammonium chloride 70, with the pH adjusted to 7.4 with 1 M TEA hydroxide.

The osmolarity of both solutions was adjusted to 290–300 mOsm/l with sucrose to reduce osmotic stress. The external solution was applied to the perfusion chamber via a gravity-fed perfusion system and the flow rate maintained at 0.5 ml/min using a Gilmont flowmeter (Barrington, IL, USA). Data were recorded at room temperature (22–25°C) which did not fluctuate more than 1°C during the course of an experiment. In all voltage-clamp experiments, the holding potential was −80 mV and the sodium concentration of the external solution was reduced to 30 mM to improve series resistance compensation and to avoid saturation in the recording system [16]. Inverted voltage-clamp command pulses were applied to the bath through a Ag/AgCl pellet/3 M KCl-agar bridge. The liquid junction potential between internal and external solutions was approximately −6 mV, and all data were compensated for this value.

Large round light DRG cells with diameters of 20–40 μm were selected for experiments. Larger cells from older animals tended to express fast TTX-sensitive sodium currents whilst smaller cells tended to express predominantly slow TTX-resistant sodium currents [20]. In those experiments that assessed the actions of δ-ACTX-Hv1b on TTX-resistant currents, 200 nM TTX was applied in the external solution to eliminate any residual TTX-sensitive sodium currents. Only those cells which exhibited less than 10% TTX-resistant sodium current, as determined from differences in the steady-state sodium channel inactivation profile, were used to determine the actions of δ-ACTX-Hv1b on TTX-sensitive sodium currents. After breaking through the membrane, experiments did not commence for a period of 20–30 min to allow for the complete block of calcium and potassium currents and any fast time-dependent shifts in steady-state sodium channel inactivation. The experiments used in this study were rejected if there were large leak currents or currents showed signs of poor space clamping such as an abrupt activation of currents upon relatively small depolarising pulses.

Stimulation and recording were both controlled by a pClamp® data acquisition system (Axon Instruments). Data were filtered at 5 kHz (4 pole low-pass Bessel filter) and digital sampling rates were between 15 and 25 kHz depending on the voltage protocol length. Leakage and capacitive currents were digitally subtracted with *P–P/4* procedures [1] and series resistance compensation was set at >80% for all cells. Data analyses were performed off-line following completion of the experiment. Mathematical curve fitting employed algorithms available in KaleidaGraph® for Macintosh using a non-linear least squares method.

The curve fits for the *I/V* data were obtained using the following equation:

$$I_{Na} = g_{max}\left(1-\left(\frac{1}{1+\exp[(V-V_{1/2})/s]}\right)\right)(V-V_{rev}) \quad (1)$$

where I_{Na} is the amplitude of the peak Na^+ current at a given test potential, V; g_{max} is the maximal Na^+ conductance; $V_{1/2}$ is the voltage at half-maximal activation; s is the slope factor and V_{rev} is the reversal potential.

The fitted curves for steady-state sodium current inactivation (h_8) were obtained using the following form of the Boltzmann equation:

$$h_8 = \frac{1-C}{1+\exp[(V-V_{1/2})/k]} + C \quad (2)$$

where $V_{1/2}$ is the voltage at half-inactivation; k is the slope factor; V is the test voltage and C is a constant or non-inactivating fraction (usually zero in controls).

Comparisons of two sample means were made using a paired Student's *t*-test. A test was considered to be significant when $P < 0.05$. All data are presented as mean ± S.E.M.

2.4. Insect toxicity assays

Insect toxicity was determined by lateroventral thoracic injection of δ-ACTX-Hv1b into third–fourth instar cricket nymphs (*Acheta domesticus* Linnaeus), as described previously [2], at doses up to 2000 pmol/g. Control crickets were injected with insect saline. Insects were monitored for 72 h following injection.

3. Results

3.1. Venom separation and toxin purification

Fig. 1A shows a rpHPLC chromatogram of pooled male and female *H. versuta* venom. The elution profile was reproducible for batches of venom, although several minor peaks that were evident in the mixed venom were not present in venom obtained exclusively from female spiders. We previously estimated that the venom contains approximately 100

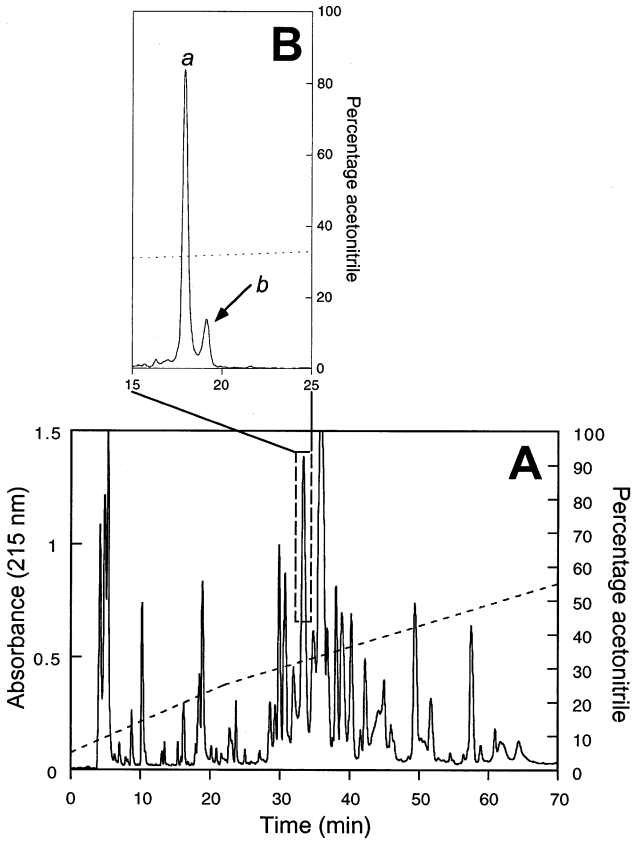

Fig. 1. rpHPLC chromatogram of pooled male and female *H. versuta* venom. (A) Screening of venom fractions revealed that the boxed peak caused spontaneous contractions of isolated rat vas deferens. (B) Further rpHPLC purification of this fraction yielded two peaks, the smaller of which (peak b) was found to be the active component in the rat vas deferens assay.

compounds, since mass spectral analyses revealed that some peaks which appear to be homogeneous by rpHPLC are actually a mixture of several components [25].

The boxed peak highlighted in Fig. 1A was found to enhance muscular contractions as well as cause spontaneous contractions of isolated rat vas deferens smooth muscle (data not shown) similar to those elicited by δ-ACTX-Ar1 [9]. Further purification of this fraction using C_{18} rpHPLC with a shallow acetonitrile gradient yielded two distinct components. The minor peak, labeled peak b in Fig. 1B, was subsequently shown to be the active component in the rat vas deferens assay. The molecular mass of peak b was determined to be 4770 Da using electrospray mass spectrometry.

3.2. Determination of amino acid sequence

Peak b was reduced and the cysteines pyridylethylated in preparation for N-terminal amino acid sequencing. This was done for two reasons. First, mass spectrometric analysis of the reduced and pyridylethylated toxin reveals the number of cysteine residues in the toxin as the mass increases by 106 Da for every cysteine residue modified with 4-vinylpyridine. Secondly, unlike unmodified phenylthiohydantoin (PTH)-Cys, PTH-Cys with a pyridylethylated sidechain is stable during automated N-terminal amino acid sequencing and therefore allows positive identification of Cys residues.

Mass spectral analysis of the pyridylethylated toxin indicated that it contained eight cysteine residues. The amino acid sequence of the toxin (see Fig. 2), obtained in a single sequencing run without the need to resort to proteolytic digestion, revealed that it contains 42 residues, including eight cysteines. The predicted mass of 4770.5 Da for the fully oxidised peptide, in which the eight cysteine residues form four disulfide bonds, is consistent with the mass spectral analysis.

A search for homologous proteins in the protein and DNA databases revealed significant homology with two other Australian funnel-web spider toxins, δ-ACTX-Hv1 [2] isolated from the same spider venom, and δ-ACTX-Ar1 [21] isolated from the venom of the Sydney funnel-web spider, *A. robustus*. The sequence shows conservation in the number and spacing of cysteine residues. When conservative substitutions are taken into consideration, the homology with δ-ACTX-Hv1 and δ-ACTX-Ar1 is 79% and 76%, respectively. The toxin has 14 amino acid substitutions relative to δ-ACTX-Hv1, whereas δ-ACTX-Hv1 and δ-ACTX-Ar1 only differ at seven positions (see Fig. 2).

Based on the sequence homology and functional similarities (see below) with δ-ACTX-Hv1, we have named the toxin δ-ACTX-Hv1b in accordance with the nomenclature previously described for toxins isolated from Australian funnel-web spiders [5]. Accordingly, in the future, δ-ACTX-Hv1 should more correctly be referred to as δ-ACTX-Hv1a. The sequence of δ-ACTX-Hv1b has been deposited in the SWISS-PROT databank under accession number P81885.

3.3. Effects of δ-ACTX-Hv1b on voltage-gated sodium currents

Under voltage-clamp conditions, δ-ACTXs have been previously shown to cause a concentration-dependent reduction in peak TTX-sensitive sodium current amplitude and slowing

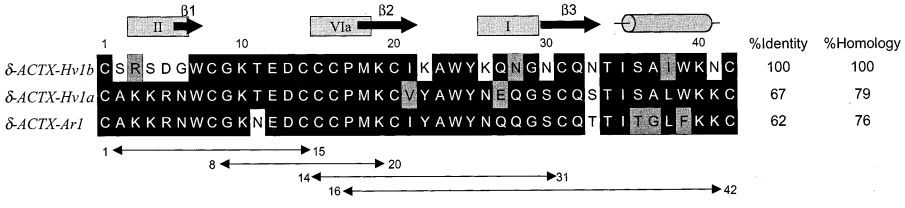

Fig. 2. Comparison of the amino acid sequences of δ-ACTX-Hv1a, δ-ACTX-Hv1b and δ-ACTX-Ar1. Identical residues are shaded in black and conservatively substituted residues are shaded in grey. The disulfide bonding pattern for the strictly conserved cysteine residues determined for δ-ACTX-Hv1a [4] and δ-ACTX-Ar1 [17] is indicated below the sequences; it is assumed that δ-ACTX-Hv1b has the same disulfide bonding pattern. Secondary structure for δ-ACTX-Hv1a is shown at the top of the figure where shaded squares represent β-turns, black arrows represent β-strands and the grey cylinder represents a 3_{10} helix [4]. δ-ACTX-Hv1b clearly belongs to the δ-ACTX family of funnel-web toxins that modulate voltage-gated sodium channels. The percentage identity and homology with δ-ACTX-Hv1b is shown to the right of the sequences.

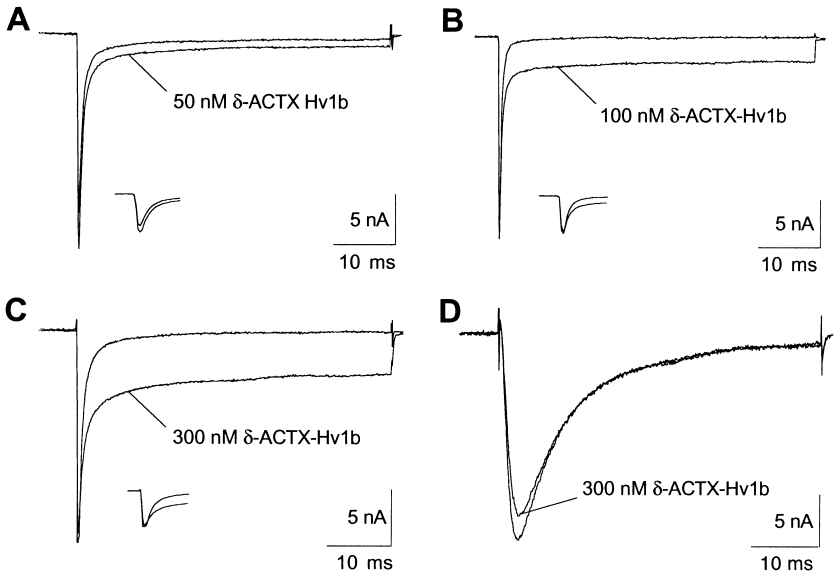

Fig. 3. Effects of δ-ACTX-Hv1b on TTX-sensitive and TTX-resistant sodium currents in rat DRG neurones. Superimposed current traces recorded following a depolarisation to −10 mV from a holding potential of −80 mV before (unlabeled) and 10 min after (labeled) the addition of toxin. (A–C) Effects of: (A) 50 nM, (B) 100 nM and (C) 300 nM δ-ACTX-Hv1b on TTX-sensitive sodium currents. Note the slowed sodium current inactivation kinetics; insets in (A–C) show the magnified peak TTX-sensitive sodium currents. (D) Effects of 300 nM δ-ACTX-Hv1b on TTX-resistant sodium currents elicited by the same stimulus protocol. Both current responses were recorded in the presence of 200 nM TTX to eliminate residual TTX-sensitive sodium currents.

of sodium current inactivation [14,15]. Fig. 3A–C shows the effect of increasing concentrations of δ-ACTX-Hv1b on TTX-sensitive sodium currents. At 300 nM, δ-ACTX-Hv1b reduced peak TTX-sensitive sodium current amplitude by 17.3 ± 4.9% ($n = 7$) and slowed the rate of TTX-sensitive sodium current inactivation. Analysis of the toxin effect on inactivation was estimated by measuring the current remaining after 50 ms following a step depolarisation to indicate the proportion of channels with permanently modified inactivation. At −10 mV, the remaining current was 11.3 ± 2.6% ($n = 7$) of control peak current. Since the threshold concentration for these actions on TTX-sensitive sodium channels in DRG neurones was found to be approximately 30 nM for δ-ACTX-Hv1b and 1–2 nM for δ-ACTX-Hv1a [15], we conclude that δ-ACTX-Hv1b is 15–30 times less potent than δ-ACTX-Hv1a on TTX-sensitive sodium channels. Similar to δ-ACTX-Hv1a, the reduction in sodium current amplitude and slowing of current inactivation produced by δ-ACTX-Hv1b was partially reversible after prolonged washing with toxin-free solution. In marked contrast to its action on TTX-sensitive sodium channels δ-ACTX-Hv1b (300 nM), like other δ-ACTXs [14,15], failed to significantly alter either the amplitude or time course of TTX-resistant sodium currents (Fig. 3D).

3.4. Effects of δ-ACTX-Hv1b on the voltage dependence of sodium channel activation

Previous studies have shown that δ-ACTXs shift the threshold of activation of TTX-sensitive sodium currents in the hyperpolarising direction [14,15]. Analysis of the I/V relationship of TTX-sensitive sodium current in the presence of 300 nM δ-ACTX-Hv1b (Fig. 2D) revealed similar 10 mV hyperpolarising shifts in the threshold of sodium channel activation. Data were normalised and fitted using a single Boltzmann distribution. δ-ACTX-Hv1b only caused a modest 6.3 mV hyperpolarising shift in the voltage midpoint ($V_{1/2}$) from −38.4 ± 1.7 mV to −44.7 ± 3.2 mV ($n = 5$) with no change in the slope factor s. Fig. 4E also shows that there was no alteration in reversal potential. These changes could not be explained by spontaneous time-dependent shifts in the voltage dependence of activation, which in general are < 5 mV in DRG neurones (G. Nicholson, unpublished results).

3.5. Effects of δ-ACTX-Hv1b on the voltage dependence of steady-state sodium channel inactivation (h_∞)

It has previously been noted that δ-ACTXs shift the steady-state sodium channel inactivation curve (h_∞/V) in the hyperpolarising direction and produce a non-inactivating component at depolarised prepulse test potentials [14,15]. To quantitate changes in the voltage dependence of steady-state sodium channel inactivation produced by δ-ACTX-Hv1b, measurements were made with a standard two-pulse protocol as detailed in Fig. 5. Peak sodium currents recorded during each test pulse were normalised to the maximum peak current and plotted against the conditioning prepulse potential. Curves were then fitted using Eq. 2. As for δ-ACTX-Hv1a and -Ar1, δ-ACTX-Hv1b caused a significant 9 mV hyperpolarising shift in the voltage at which half the sodium channels were inactivated ($V_{1/2}$) from −58.0 ± 0.7 mV to −67.1 ± 0.8 mV (paired Student's t-test, $P < 0.02$, $n = 4$) with no change in the slope factor. In addition, 300 nM δ-ACTX-Hv1b exhibited a classical non-inactivating component (8.6 ± 1.2% of the maximal sodium current, determined from C in Eq. 2) at prepulse test potentials more depolarised than −40 mV.

3.6. Insecticidal potency of δ-ACTX-Hv1b

δ-ACTX-Hv1a was previously shown to be a moderately potent insecticidal toxin, with an LD_{50} of 770 pmol/g in house crickets (*A. domesticus*) [11]. Furthermore, δ-ACTX-Hv1a caused contractile paralysis at significantly lower doses

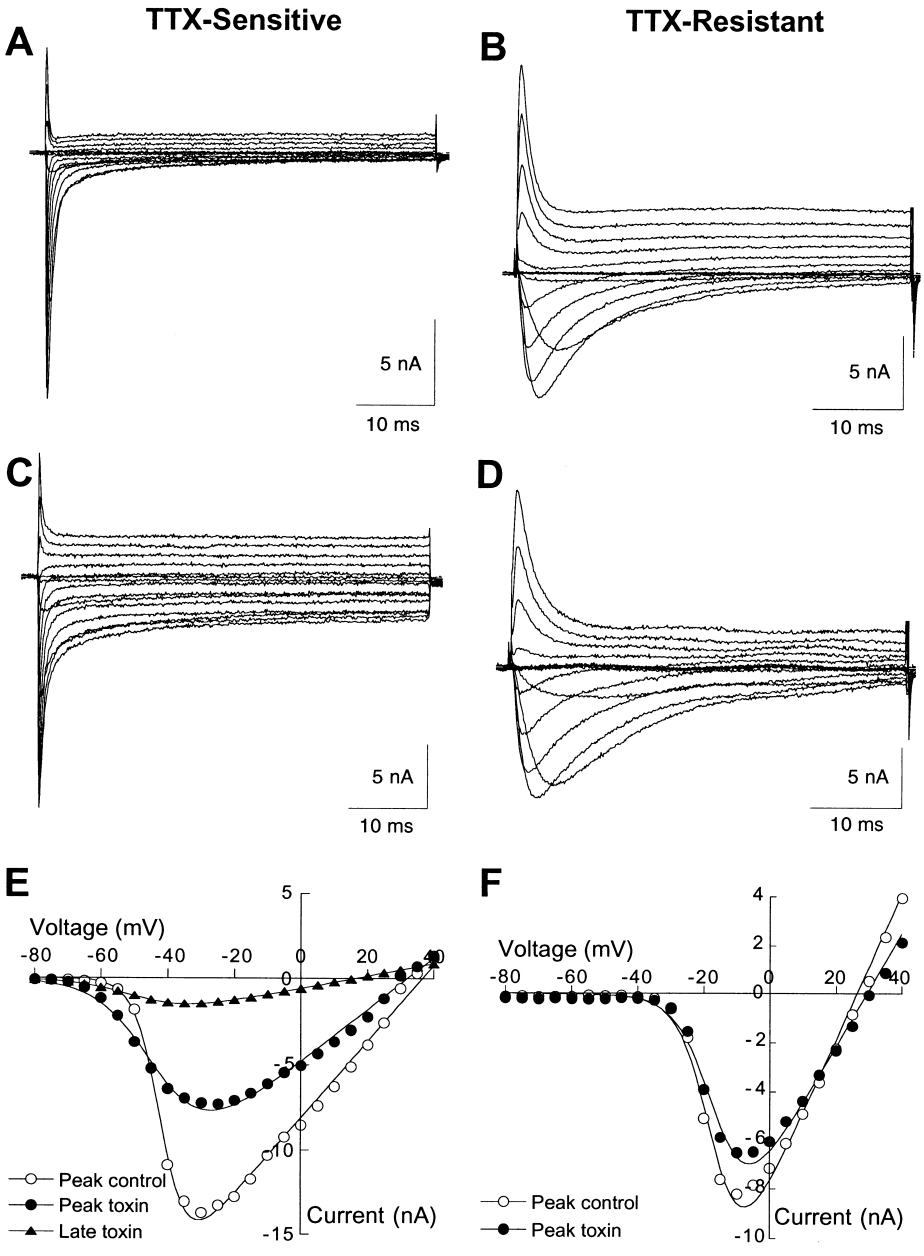

Fig. 4. Typical effects of δ-ACTX-Hv1b on the current–voltage (*I*/*V*) relationship. Families of sodium currents were evoked by a series of 50 ms depolarisations from −80 to +70 mV in 5 mV steps applied every 10 s from a holding potential of −80 mV. Left-hand panels show effects on TTX-sensitive sodium currents while right-hand panels show effects on TTX-resistant sodium currents recorded in the presence of 200 nM TTX. (A–D) Families of sodium currents before (A,B) and after (C,D) application of 300 nM δ-ACTX-Hv1b. For clarity, sodium currents recorded in 10 mV steps are presented. Note that the inactivation kinetics of both inward and outward currents are slowed and incomplete in (C) only. (E,F) Peak (circles) and late (triangles) *I*/*V* relationships are shown before (empty symbols) and following (filled symbols) a 10 min perfusion with 300 nM δ-ACTX-Hv1b. Late currents were measured at the end of each 50 ms depolarising test pulse. Peak and late currents were fitted according to Eq. 1 described in Section 2.

(PD_{50} = 200 pmol/g), with the higher LD_{50} reflecting the fact that most crickets recover from the contractile paralysis at doses near or below the PD_{50} [11]. Surprisingly, no adverse effects (i.e. neither paralysis nor death) were observed in crickets in the 72 h following injection of δ-ACTX-Hv1b at doses up to 2000 pmol/g (i.e. 10 times the PD_{50} for δ-ACTX-Hv1a). Thus δ-ACTX-Hv1b completely lacks insecticidal activity in the same assay system despite strong sequence similarity with δ-ACTX-Hv1a.

4. Discussion

We recently embarked on a rational screening of all peptidic components in the venom of *H. versuta* (G.F.K. et al., unpublished results). Initial screening of crude venom fractions using a rat vas deferens bioassay revealed a fraction that produced spontaneous contractions similar to those seen with δ-ACTX-Hv1a previously isolated from the venom of the same spider. As described here, further purification of

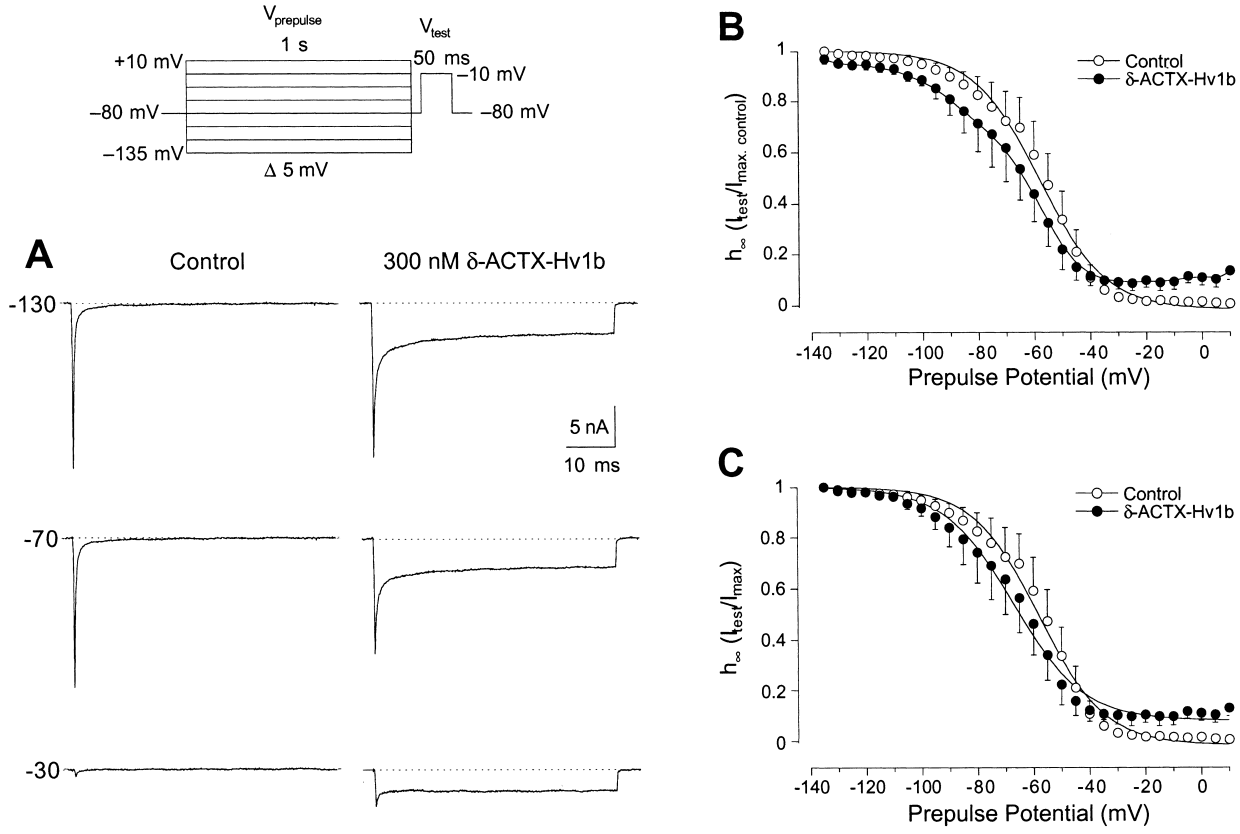

Fig. 5. Effects of δ-ACTX-Hv1b on steady-state TTX-sensitive sodium current inactivation (h_∞). Steady-state inactivation was determined using the two-pulse protocol shown in the inset. Conditioning prepulse voltages of 1 s duration ranging from −135 to +10 mV in 5 mV steps were delivered every 10 s. (A) Typical current traces obtained following a 50 ms test pulse to −10 mV subsequent to prepulse potentials of −130, −70 and −30 mV before (left-hand traces) and following a 10 min perfusion with 300 nM δ-ACTX-Hv1b (right-hand traces). The dashed line represents the zero current level. (B) Peak sodium currents are plotted against prepulse potential with currents normalised to the maximum control current. The amount of sodium current that is available for activation during the test pulse under control conditions (open circles) and during 300 nM δ-ACTX-Hv1b (closed circles) is shown. Note that, despite a hyperpolarising shift in h_∞, 96.8 ± 1.9% of maximum control current could be achieved at a holding potential of −135 mV in the presence of 300 nM δ-ACTX-Hv1b. (C) Currents were normalised to the maximum current recorded under control conditions (open circles) or in the presence of 300 nM δ-ACTX-Hv1b (closed circles). Data in (C) were fitted according to Eq. 2 described in Section 2. Data represent the mean ± S.E.M. of four experiments.

the crude venom fraction and subsequent N-terminal sequencing showed that the active component, which we have designated δ-ACTX-Hv1b, corresponds to a 42 residue peptide of molecular weight 4770 Da which is clearly a homologue of δ-ACTX-Hv1a.

Given that previously characterised δ-ACTXs are potent modulators of sodium channel inactivation [14,15], we characterised the mode of action of δ-ACTX-Hv1b on sodium channel gating and kinetics. The findings of this study demonstrate that this novel toxin has selective effects on TTX-sensitive sodium currents including: (a) a slowing of channel inactivation; (b) shifts in the voltage dependence of activation; and (c) a hyperpolarising shift in steady-state inactivation (h_∞). In contrast, TTX-resistant sodium channel gating and kinetics remained unaffected.

The main action of δ-ACTX-Hv1b is to considerably slow TTX-sensitive sodium channel inactivation as evidenced by a steady-state current maintained during depolarising test pulses. Moreover, in the presence of δ-ACTX-Hv1b, a small but significant portion of TTX-sensitive sodium currents (8%) failed to inactivate even with prolonged large depolarising prepulses to +10 mV for 1 s. δ-ACTX-Hv1b also produced a 9 mV hyperpolarising shift in the voltage dependence of steady-state inactivation (h_∞) as a consequence decreasing peak TTX-sensitive sodium current at holding potentials of −80 mV (see Fig. 3). This is most likely the result of a reduction in the availability of channels at membrane potentials of −80 mV since the maximum peak inward current recorded from holding potentials of −135 mV is not significantly reduced (see Fig. 5A). δ-ACTX-Hv1b also altered the voltage dependence of TTX-sensitive sodium channel activation by shifting the threshold of activation (Fig. 4).

These actions, especially the slowing of sodium current inactivation in the absence of large shifts in the voltage dependence of activation or profound slowing of deactivation, indicates that δ-ACTX-Hv1b acts in a manner similar to scorpion α-toxins, sea anemone toxins and previously characterised δ-ACTXs that bind to neurotoxin receptor site 3. These actions suggest that δ-ACTX-Hv1b inhibits conversion of TTX-sensitive sodium channels from the open state to the inactivated state, thus allowing a fraction of the sodium current to remain at membrane potentials where inactivation is normally complete. This is qualitatively similar to other δ-ACTXs, although δ-ACTX-Hv1b appears to be approximately 15–30-fold less potent in its modulation of sodium channel gating and kinetics.

Unfortunately, the presence of the four disulfide bonds has severely limited the efficient production of synthetic or recombinant δ-ACTXs in order to assess the effect of mutations. Therefore, the structure–function relationships, in particular the channel-binding surface, of these toxins are at present unknown. However, the mutagenesis study of Rogers et al. [19] has identified a number of residues in the S3–S4 short extracellular loop of domain IV of the sodium channel α-subunit critical for the binding of scorpion α-toxins and sea anemone toxins. Those residues identified as critical for binding (Glu-1613, Glu-1616 and Lys-1617) are all charged, consistent with the identification of several anionic and cationic residues in scorpion α-toxins and sea anemone toxins that are crucial for binding to neurotoxin receptor site 3 of the sodium channel [10,13]. Fletcher et al. [4] found that three cationic and two anionic residues in δ-ACTX-Hv1a can be superimposed on similarly charged residues in the structures of anthopleurin-B and Aah II, despite their lack of sequence homology and totally different three-dimensional folds. They proposed that Lys-3, Arg-5 and Asp-13 in δ-ACTX-Hv1a provide a complementary surface to the residues identified in the S3–S4 loop of domain IV. In the absence of mutational studies of δ-ACTXs, it would therefore appear that these three residues are important for mammalian toxicity.

Importantly δ-ACTX-Hv1a/Ar1 also show insect toxicity and compete for LqhαIT-binding [11]. Despite their completely different three-dimensional folds, the structures of δ-ACTX-Hv1a and LqhαIT can be similarly overlaid such that residues Lys-4, Arg-5 and Lys-19 in δ-ACTX-Hv1a superimpose very closely on residues Arg-64, Lys-62 and Lys-8 in LqhαIT [11]. Interestingly, these residues are different to those that superimpose on the structures of Aah II and anthopleurin-B.

δ-ACTX-Hv1b is unique amongst the δ-ACTXs in that it lacks insecticidal activity and shows a 15–30-fold reduction in mammalian activity compared to δ-ACTX-Hv1a/Ar1. Close inspection of the primary structure reveals that a number of charged amino acids at the N-terminus are not conserved between δ-ACTX-Hv1b and δ-ACTX-Hv1a/Ar1 (see Fig. 2). Since the two N-terminal cationic residues (Lys-4 and Arg-5) are substituted by Ser-4 and Asp-5 in δ-ACTX-Hv1b, this lends support to the hypothesis that Lys-4 and Arg-5 are important for insect activity. In addition, δ-ACTX-Hv1b shows considerably reduced activity on mammalian sodium channels, consistent with the non-conserved mutation at position 5.

Given that δ-ACTXs target both mammalian and insect sodium channels, they have considerable potential as tools to aid in the investigation of structural requirements for anti-insect versus anti-mammal activity. The residues that differ between δ-ACTX-Hv1b and δ-ACTX-Hv1a/Ar1 therefore give us an unexpected insight into the residues that facilitate interaction of δ-ACTXs with insect sodium channels. This raises the possibility that manipulation of key residues may enable construction of a functional mirror-image of δ-ACTX-Hv1b, namely a δ-ACTX that works on insect, but not vertebrate, voltage-gated sodium channels. Such an insect-specific δ-ACTX might be a useful biopesticide.

Acknowledgements: This work was supported by Australian Research Council research grants to G.F.K., M.J.C. and G.M.N. and a University of Technology, Sydney, research grant to G.M.N. The authors would like to thank Ms Cathy Zappia for assistance with the maintenance and milking of the funnel-web spider colony. We are also grateful to the general public and councils and hospitals in the following shires for kind donations of spiders: Baulkham Hills, Gosford, Hornsby, Hunters Hill, Hurstville, Kuring-gai, Lane Cove, Manly, North Sydney, Parramatta, Pittwater, Sutherland, Warringah, Willoughby, Wollondilly and Wollongong.

References

[1] Bezanilla, F. and Armstrong, C.M. (1977) J. Gen. Physiol. 70, 566–594.
[2] Brown, M.R., Sheumack, D.D., Tyler, M.I. and Howden, M.E.H. (1988) Biochem. J. 250, 401–405.
[3] Eitan, M., Fowler, E., Herrmann, R., Duval, A., Pelhate, M. and Zlotkin, E. (1990) Biochemistry 29, 5941–5947.
[4] Fletcher, J.I., Chapman, B.E., Mackay, J.P., Howden, M.E.H. and King, G.F. (1997) Structure 5, 1525–1535.
[5] Fletcher, J.I., Smith, R., O'Donoghue, S.I., Nilges, M., Connor, M., Howden, M.E.H., Christie, M.J. and King, G.F. (1997) Nat. Struct. Biol. 4, 559–566.
[6] Fontecilla-Camps, J.C., Almassy, R.J., Suddath, F.L. and Bugg, C.E. (1982) Toxicon 20, 1–7.
[7] Hamill, O.P., Marty, A., Neher, E., Sakmann, B. and Sigworth, F.J. (1981) Pflüg. Arch. (Eur. J. Physiol.) 391, 85–100.
[8] Hanck, D.A. and Sheets, M.F. (1995) J. Gen. Physiol. 106, 601–616.
[9] Harris, J.B., Sutherland, S.K. and Zar, M.A. (1981) Br. J. Pharmacol. 72, 335–340.
[10] Housset, D., Habersetzer-Rochat, C., Astier, J.P. and Fontecilla-Camps, J.C. (1994) J. Mol. Biol. 238, 88–103.
[11] Little, M.J., Wilson, H., Zappia, C., Cestèle, S., Tyler, M.I., Martin-Eauclaire, M.-F., Gordon, D. and Nicholson, G.M. (1998) FEBS Lett. 439, 246–252.
[12] Little, M.J., Zappia, C., Gilles, N., Connor, M., Tyler, M.I., Martin-Eauclaire, M.-F., Gordon, D. and Nicholson, G.M. (1998) J. Biol. Chem. 273, 27076–27083.
[13] Monks, S.A., Pallaghy, P.K., Scanlon, M.J. and Norton, R.S. (1995) Structure 3, 791–803.
[14] Nicholson, G.M., Walsh, R., Little, M.J. and Tyler, M.I. (1998) Pflüg. Arch. (Eur. J. Physiol.) 436, 117–126.
[15] Nicholson, G.M., Willow, M., Howden, M.E.H. and Narahashi, T. (1994) Pflüg. Arch. (Eur. J. Physiol.) 428, 400–409.
[16] Ogata, N., Nishimura, M. and Narahashi, T. (1989) J. Pharmacol. Exp. Ther. 248, 605–613.
[17] Pallaghy, P.K., Alewood, D., Alewood, P.F. and Norton, R.S. (1997) FEBS Lett. 419, 191–196.
[18] Pallaghy, P.K., Neilsen, K.J., Craik, D.J. and Norton, R.S. (1993) Protein Sci. 3, 1833–1839.
[19] Rogers, J.C., Qu, Y., Tanada, T.N., Scheuer, T. and Catterall, W.A. (1996) J. Biol. Chem. 271, 15950–15962.
[20] Roy, M.L. and Narahashi, T. (1992) J. Neurosci. 12, 2104–2111.
[21] Sheumack, D.D., Claassens, R., Whiteley, N.M. and Howden, M.E.H. (1985) FEBS Lett. 181, 154–156.
[22] Strichartz, G.R. and Wang, G.K. (1986) J. Gen. Physiol. 88, 413–435.
[23] Szeto, T.H., Wang, X.-H., Smith, R., Connor, M., Christie, M.J., Nicholson, G.M. and King, G.F. (2000) Toxicon 38, 429–442.
[24] Tugarinov, V., Kustanovich, I., Zilberberg, N., Gurevitz, M. and Anglister, J. (1997) Biochemistry 36, 2414–2424.
[25] Wang, X.-H., Smith, R., Fletcher, J.I., Wilson, H., Wood, C.J., Howden, M.E.H. and King, G.F. (1999) Eur. J. Biochem. 264, 488–494.